PAPER • OPEN ACCESS

Preliminary symptoms assessment of typical faults related to the fans and humidifiers of HVAC systems based on experimental data collected during Italian summer and winter

To cite this article: A Rosato *et al* 2021 *IOP Conf. Ser.: Earth Environ. Sci.* **897** 012009

View the article online for updates and enhancements.

You may also like

- Effects of increasing urban albedo in the Greater Toronto Area
Jandaghian Zahra and Berardi Umberto
- System solution to improve energy efficiency of HVAC systems
L Chretien, R Becerra, N P Salts et al.
- Problems and Improvement Methods of HVAC Design of Building
Ruan Xiaolong

This content was downloaded from IP address 5.170.141.169 on 03/01/2022 at 10:36

IOP Conf. Series: Earth and Environmental Science **897** (2021) 012009 doi:10.1088/1755-1315/897/1/012009

Preliminary symptoms assessment of typical faults related to the fans and humidifiers of HVAC systems based on experimental data collected during Italian summer and winter

A Rosato[1,*], F Guarino[1,*], M El Youssef[1], S Sibilio[1] and L Maffei[1]

[1]Department of Architecture and Industrial Design, University of Campania Luigi Vanvitelli, Via San Lorenzo 4, 81031 Aversa, Italy

antonio.rosato@unicampania.it, francesco.guarino@unicampania.it

Abstract. The symptoms associated to the occurrence of typical faults in a heating, ventilation and air-conditioning (HVAC) system, including a single duct dual fan constant air volume air-handling unit, have been experimentally characterized. The operation of the HVAC unit with 3 artificially forced faults ((1) reduced velocity of the supply air fan, (2) reduced velocity of the return air fan, (3) the valve supplying the humidifier kept always closed) has been analysed and compared with that of healthy operation of the same plant under very similar boundary conditions (outside air temperature and initial indoor air temperature) during Italian summer and winter in order to preliminarily assess (i) the effects on the main operating parameters, and (ii) generate preliminary operation data to assist further research in fault detection and diagnosis of HVAC systems.

1. Introduction

The building sector plays a vital role in reducing greenhouse gases (GHG) emissions. In 2017, globally, the building sector accounted for 21% of the world's final energy use and it was responsible for 17% of the world's total energy-related GHG emissions [1]. Heating, ventilation and air-conditioning (HVAC) systems account for almost 50% of building energy consumption and about 10-20% of total energy demand in developed countries [2]. The integration of renewable energy sources into HVAC units is considered as one of the best options to reduce fossil fuel demand and, thus, related GHG emissions [3]. HVAC systems are often run under faulty conditions due to lack of proper maintenance, failure of components or incorrect installation. A study conducted on more than 55.000 Air Handling Units (AHUs) showed that a fraction of 90% runs with one or multiple faults [4]. Lin et al. [5] estimated that an effective identification and diagnosis of the faults in HVAC systems could save from 15% to 30% of the total energy consumed by buildings. Automated Fault detection and diagnosis (AFDD) is an automated process of detecting deviations from normal or expected operation (faults) and diagnosing the type of problem or its location [6-8]. AFDD technologies can offer several interrelated benefits, including energy savings and improved operational efficiency, utility cost savings, streamlining operations and maintenance processes as well as support for continuous energy management practices [5-7]. AFDD strategies represent one of the most active areas of research as well as a very fast-growing market segment in the context of building analytics technologies [5-7]. The methods used for performing AFDD analyses can be classified in (i) quantitative model-based, (ii)

Content from this work may be used under the terms of the Creative Commons Attribution 3.0 licence. Any further distribution of this work must maintain attribution to the author(s) and the title of the work, journal citation and DOI.
Published under licence by IOP Publishing Ltd

qualitative model-based and (iii) data driven-based [5,7]. The last category includes methodologies exploiting operational data collected from the system under investigation [5,7]. Data-driven AFDD approaches have gained encouraging results thanks to their flexibility in practical applications as well as the developments in data analytics [5,6]; nevertheless, the adoption of data-driven AFDD models is mainly limited by the lack of labelled data due to the fact that the architecture of sensor networks in HVAC units is not designed for AFDD purposes and, therefore, some important variables are generally not measured. Even if several scientific works focusing on data-driven AFDD methods are available in current literature [6,7], most of them refer to the ASHRAE RP-1312 data set dated 2011 [9]; relatively few studies give detailed information on how the faults are experimentally implemented in a real HVAC system or modelled [7,9]; even fewer studies describe how their simulated faulty operation data are validated [7,9]; nearly all the studies only consider one HVAC operation condition with changing weather conditions [9]; not many studies quantitatively examine how various faults and fault severities impact energy consumption, user comfort, maintenance cost and equipment life cycle [9]. According to [5], additional works to characterize the faults' prevalence based on field empirical data could prove valuable in guiding future AFDD development and implementation efforts. Lin et al [5] also highlighted that future AFDD studies should focus on expansion of test datasets as well as their provision for public use. In this paper, the symptoms associated to the occurrence of typical faults in the HVAC system serving the integrated test room of the SENS i-Lab of the Department of Architecture and Industrial Design of the University of Campania Luigi Vanvitelli (Aversa, south of Italy) have been experimentally characterized. The operation of the system with 3 artificially forced faults ((1) reduced velocity of supply air fan, (2) reduced velocity of return air fan, (3) humidifier valve kept always closed) has been analysed and compared with that of healthy operation of the same plant under similar boundary conditions (outside air temperature and initial indoor air temperature) during summer and winter. The analysis has been performed with the aim of (i) preliminarily assessing the effects on key operating parameters, and (ii) generating preliminary operation data to assist further research in fault detection and diagnosis of HVAC systems.

2. Description of the experimental set-up

The SENS i-Lab is an innovative, multi-sensorial and multi-purpose laboratory of the Department of Architecture and Industrial Design of the University of Campania Luigi Vanvitelli (Aversa, south of Italy, latitude: 40°58'21" N, longitude: 14°12'26" E). It mainly consists of an integrated test room served by a typical HVAC system, including a single duct dual fan constant air volume air-handling unit, able to control indoor air temperature, indoor air relative humidity, indoor air velocity and indoor air quality. The integrated test room is characterized by a floor area of 16.0 m^2, with a height of 3.6 m. Figure 1 reports the schematic of the AHU.

Table 1 describes the main characteristics of the AHU components. The heat carrier fluid is a mixture of water and ethylene glycol (90%/10% by volume). The AHU also includes the return air damper (D_{RA}), the outside air damper (D_{OA}), the exhaust air damper (D_{EA}) and the heat-recovery system damper (D_{HRS}). Three-way valves (V_{PreHC}, V_{PostHC}, V_{CC} and V_{HUM}) supply the pre-heating coil, the post-heating coil, the cooling coil and the humidifier, respectively.

The AHU is fully equipped in order to monitor, control and record the key parameters of the system. The main characteristics of the AHU sensors are reported in table 2. The AHU is operated according to a specific control logic. The following parameters are manually set (and eventually modified during the test) by end-users: (i) the desired targets of both indoor air temperature ($T_{SP,Room}$) and relative humidity ($RH_{SP,Room}$) to be achieved inside the test room; (ii) the deadbands DB_T and DB_{RH} for both $T_{SP,Room}$ and $RH_{SP,Room}$, respectively; (iii) the velocity of both the return air fan (OL_{RAF}) and the supply air fan (OL_{SAF}); (iv) the opening percentages of the return air damper (OP_{DRA}), the outside air damper (OP_{DOA}) and the exhaust air damper (OP_{DEA}); (v) the activation of the static heat recovery system damper (OP_{DHRS}). Once the previous parameters are manually set by end-users, the opening percentages (OP_{V_PreHC}, OP_{V_PostHC}, OP_{V_CC} and OP_{V_HUM}) of the valves supplying the pre-heating coil, the post-heating coil, the cooling coil and the humidifier are automatically managed in the range 0÷100% by PID (proportional-integral-derivative) controllers in order to achieve the desired targets inside the test room. However, alternatively the end-users are allowed to alter the components' operation based on specific research purposes by manually forcing (at the beginning or during the test) the opening percentages of the valves supplying the pre-heating coil, the post-heating coil, the cooling coil and the humidifier.

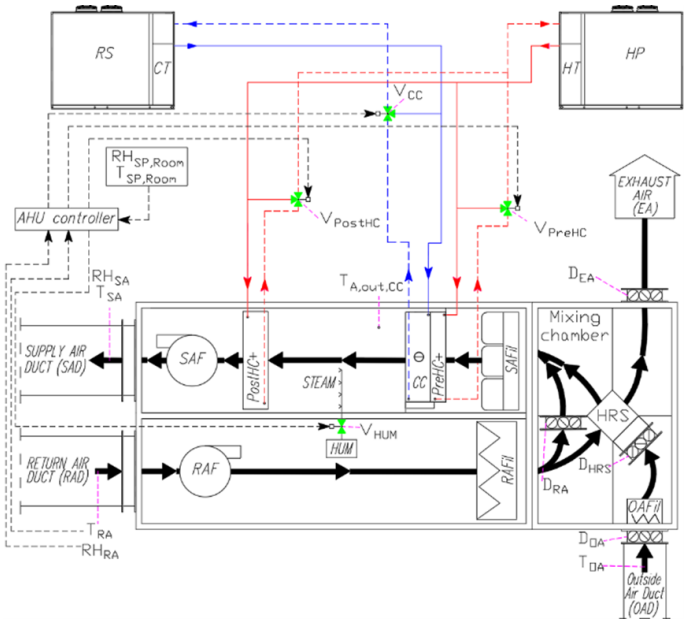

Figure 1. Schematic of the AHU.

Table 1. Characteristics of the main AHU components.

Supply air fan (SAF)/Return air fan (RAF)	Nominal supply/return air flow rate (m^3/h)	600/600
Cross flow heat recovery system (HRS)	Nominal efficiency (%)/recovery capacity (kW)	74.7/3.1
Pre-heating coil (PreHC)	Nominal heating capacity (kW) Nominal heat carrier fluid/air flow rate (m^3/h)	4.1 0.71/600
Cooling coil (CC)	Nominal cooling capacity (kW) Nominal heat carrier fluid/air flow rate (m^3/h)	5.0 0.86/600
Humidifier (HUM)	Nominal steam capacity (kg/h)/power (kW)	5.0/3.7
Post-heating coil (PostHC)	Nominal heating capacity (kW) Nominal heat carrier fluid/air flow rate (m^3/h)	5.0 0.86/600
Heat pump (HP)/Refrigerating system (RS)	Nominal capacity (kW) Nominal input power (kW) Nominal heat carrier fluid flow rate (m^3/h)	14.0/13.4 4.75/4.48 2.41/2.31

Table 2. Characteristics of the AHU sensors.

Monitored Parameter	**Measuring range**	**Accuracy**
Return air temperature T_{RA} / Supply air temperature T_{SA}	0 ÷ 50 °C	±0.8 K
Return air relative humidity RH_{RA} / Supply air relative humidity RH_{SA}	0 ÷ 100%	±3%
Outside air temperature T_{OA} / Cooling coil outlet air temperature $T_{A,out,CC}$	-50 ÷ 50 °C	±0.75 K

The refrigeration device operates to maintain a temperature T_{CT} of 7 °C inside the 75 liters cold tank (CT), while the heat pump is activated in order to achieve a temperature T_{HT} of 45 °C inside the 75 liters hot tank (HT). Air flow rate moved by the supply air fan can be varied between 0 (OL_{SAF} = 0%) and 1080 m^3/h (OL_{SAF} = 100%), while air flow rate of the return air fan is in the range from 0 (OL_{RAF} = 0%) up to 1460 m^3/h (OL_{RAF} = 100%). The parameters OP_{DRA}, OP_{DOA} and OP_{DEA} can be varied in the range 0–100%, where 100% means that the damper is fully open. The parameter OP_{DHRS} can be set to 100% (no heat recovery) or 0% (heat recovery takes place).

3. Experimental tests

Ten fault free and faulty experiments have been carried out to preliminarily investigate the HVAC behaviour under summer and winter conditions with reference to the occurrence of 3 specific faults. Table 3 describes the operating conditions of the fault free tests, while table 4 describes the operating conditions of the faulty tests.

Table 3. Operating conditions of the fault free tests.

	S1_FF	**W1_FF**	**W2_FF**	**W3_FF**
$T_{SP,Room}$	26 °C	20 °C	20 °C	20 °C
$RH_{SP,Room}$	50 %			
DB_T	1 °C			
DB_{RH}	5 %			
OL_{SAF}	50 %			
OL_{RAF}	50 %			
OP_{V_PostHC}, OP_{V_CC}, OP_{V_HUM}	0 ÷ 100 %			
OP_{DRA}, OP_{DHRS}	100 %			
OP_{DOA}, OP_{DEA}	20 %			
Date (dd/mm/yyyy)	21/07/2020	23/12/2020	29/12/2020	05/01/2021

Table 4. Operating conditions of the faulty tests.

	S2_F1	**S3_F2**	**S4_F3**	**W4_F1**	**W5_F2**	**W6_F3**
$T_{SP,Room}$	20 °C	20 °C	20 °C	26 °C	26 °C	26 °C
$RH_{SP,Room}$	50 %					
DB_T	1 °C					
DB_{RH}	5 %					
OL_{SAF}	20 %	50 %	50 %	20 %	50 %	50 %
OL_{RAF}	50 %	20 %	50 %	50 %	20 %	50 %
OP_{V_PostHC}, OP_{V_CC}	0 ÷ 100 %					
OP_{V_HUM}	0 ÷ 100 %	0 ÷ 100 %	0 %	0 ÷ 100 %	0 ÷ 100 %	0 %
OP_{DRA}, OP_{DHRS}	100 %					
OP_{DOA}, OP_{DEA}	20 %					
Date (dd/mm/yyyy)	31/07/2020	03/08/2020	18/09/2020	12/01/2021	14/01/2021	12/02/2021

Four tests (S1_FF, W1_FF, W2_FF, W3_FF) have been performed under fault free (FF) operating conditions; in more detail, the test S1_FF has been performed during the summer 2020 (S), while the other tests W1_FF, W2_FF and W3_FF have been carried out during the winter 2020/2021 (W). The remaining 6 tests (S2_F1, S3_F2, S4_F3, W4_F1, W5_F2, W6_F3) have been carried out while forcing the operation of specific AHU components (supply air fan, return air fan, humidifier valve) in order to artificially simulate 3 specific typical faults. The tests S2_F1, S3_F2 and S4_F3 have been performed during the summer 2020 (S), while the other tests W4_F1, W5_F2, W6_F3 have been carried out during the winter 2020/2021 (W). In greater detail, the fault 1 (F1), i.e. velocity of supply air fan forced at 20% (instead of the nominal value of 50%), has been artificially implemented during the tests S2_F1 and W4_F1; the fault 2 (F2), i.e. velocity of return air fan forced at 20% (instead of the nominal value of 50%), has been artificially implemented during the tests S3_F2 and W5_F2; the fault 3 (F3), i.e. opening percentage of the humidifier valve kept closed (instead of allowing its healthy operation with a value of OP_{V_HUM} in the range 0÷100%), has been artificially implemented during the tests S4_F3 and W6_F3. During all the experiments, the pre-heating coil has been always manually de-activated and the parameters indicated in table 2 have been measured every minute.

4. Comparison of boundary conditions between fault free and faulty tests

The faulty tests (S2_F1, S3_F2, S4_F3, W4_F1, W5_F2, W6_F3) have been carried out under very similar boundary conditions (i.e. outside air temperature as well as initial indoor return air temperature) with respect to the fault free tests (S1_FF, W1_FF, W2_FF, W3_FF). The fault free test S1_FF has very similar boundary conditions in comparison to the faulty tests S2_F1, S3_F2 and S4_F3 (in greater detail, the test S1_FF is longer and, therefore, different portions of the entire test S1_FF have been compared with the entire tests S2_F1, S3_F2 and S4_F3); the fault free tests W1_FF, W2_FF and W3_FF are characterized by very similar

boundary conditions with respect to the faulty tests W6_F3, W4_F1 and W5_F2, respectively. Boundary conditions of the above-mentioned fault free and faulty experiments are compared in terms of outside air temperature and initial indoor return air temperature to assess their similarity. Figures 2a, 2b and 2c compare the test S1_FF with the tests S2_F1, S3_F2 and S4_F3, respectively. Figure 2d compares the tests W2_FF and W4_F1, figure 2e compares the tests W3_FF and W5_F2 and figure 2f compares the tests W1_FF and W6_F3.

Fig. 2. Comparison of fault free and faulty tests in terms of T_{OA} and T_{RA}: comparison between S1_FF and S2_F1 (a), S1_FF and S3_F2 (b), S1_FF and S4_F3 (c), W2_FF and W4_F1 (d), W3_FF and W5_F2 (e), W1_FF and W6_F3 (f).

Figures 2a-f highlight very similar boundary conditions in terms of T_{OA} and initial T_{RA} between the corresponding fault free and faulty tests. The comparison in terms of outside air temperature has also been performed by means of the following metrics (the average difference $\bar{\varepsilon}$, the average absolute difference $|\bar{\varepsilon}|$, the root mean square difference RMSD):

$$\varepsilon_i = T_{OA,Fault\_free,i} - T_{OA,Faulty,i} \quad (1)$$

$$\bar{\varepsilon} = \sum_{i=1}^{N} \varepsilon_i / N \quad (2)$$

$$|\bar{\varepsilon}| = \sum_{i=1}^{N} |\varepsilon_i| / N \quad (3)$$

$$RMSD = \sqrt{\sum_{i=1}^{N} [(\varepsilon_i - \bar{\varepsilon})^2] / N} \quad (4)$$

where N is the number of experimental data points, while $T_{OA,Fault\_free,i}$ and $T_{OA,Faulty,i}$ are, respectively, the experimental values of outside air temperature at time step i under healthy and faulty operations. Table 5 summarizes the values of $\bar{\varepsilon}$, $|\bar{\varepsilon}|$ and RMSD as result of comparisons of the above-mentioned fault free and faulty tests. The results highlight how the values of $\bar{\varepsilon}$, $|\bar{\varepsilon}|$ and RMSD are at most 1.09 °C, 1.12 °C and 0.89

°C, respectively. Therefore, it can be stated that, according to [9], the boundary conditions of the corresponding fault free and faulty tests are very similar; as a consequence, comparing the above-mentioned healthy and faulty tests is possible for assessing the impact of each investigated fault on the AHU behavior/performance.

Table 5. Comparison of healthy and faulty tests in terms of outside air temperature T_{OA}.

Fault free against faulty tests	$\bar{\varepsilon}$ (°C)	$\overline{\lvert\varepsilon\rvert}$ (°C)	RMSD (°C)
S1_FF compared with S2_F1	-0.15	0.77	0.88
S1_FF compared with S3_F2	-0.75	0.96	0.89
S1_FF compared with S4_F3	0.44	0.67	0.80
W2_FF compared with W4_F1	0.53	0.60	0.74
W3_FF compared with W5_F2	1.09	1.12	0.70
W1_FF compared with W6_F3	0.54	0.58	0.40

5. Experimental symptoms of typical faults on HVAC performance

In Figure 3 the experimental performance of the HVAC system during the fault free and faulty tests have been compared in terms of (1) return air temperature (T_{RA}), (2) air temperature at the outlet of the cooling coil ($T_{A,out,CC}$), (3) supply air temperature (T_{SA}), (4) return air relative humidity (RH_{RA}) and (5) supply air relative humidity (RH_{SA}). In particular, figures 3a, 3b and 3c compare the test S1_FF with the tests S2_F1, S3_F2, S4_F3, respectively. Figure 3d compares the tests W2_FF and W4_F1. Figure 3e compares the tests W3_FF and W5_F2. Figure 3f compares the tests W1_FF and W6_F3.

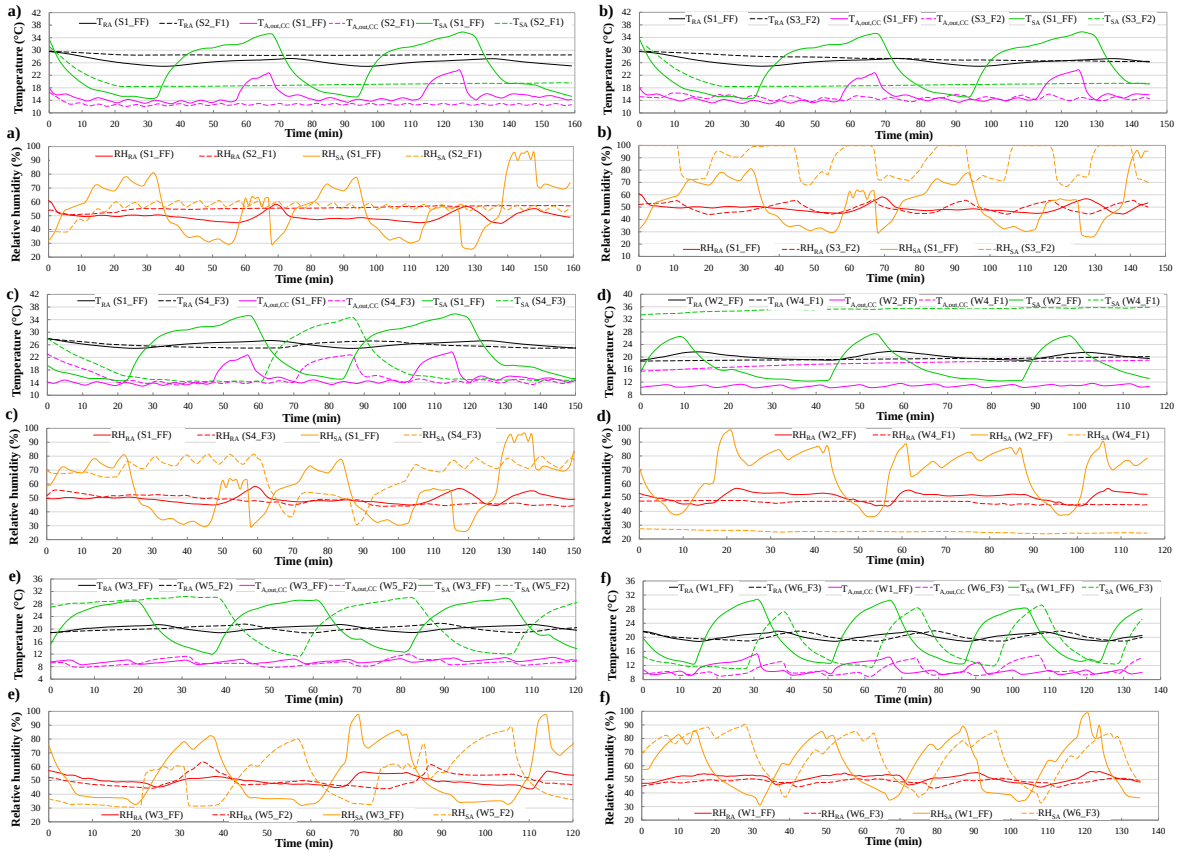

Fig. 3. Comparison of fault free and faulty tests in terms of T_{RA}, $T_{A,out,CC}$, T_{SA}, RH_{RA}, RH_{SA}: comparison between S1_FF and S2_F1 (a), S1_FF and S3_F2 (b), S1_FF and S4_F3 (c), W2_FF and W4_F1 (d), W3_FF and W5_F2 (e), W1_FF and W6_F3 (f).

The comparison between normal and faulty tests in terms of (1) $T_{A,out,CC}$, (2) T_{RA}, (3) RH_{RA}, (4) T_{SA} and (5) RH_{SA} has also been performed by contrasting the arithmetic mean μ as well as standard deviation σ of the above-mentioned 5 parameters calculated as follows:

$$\mu = \sum_{i=1}^{N} d_i / N \quad (5)$$

$$\sigma = \sqrt{\sum_{i=1}^{N} (d_i - \mu)^2 / N} \quad (6)$$

where N is the number of experimental points and d_i is the experimental value at time step i. The calculated values of μ and σ are reported in table 6; this table also shows the percentage difference %D between the arithmetic mean and the standard deviation of each above-mentioned parameters calculated during a faulty test with respect to those obtained during the similar fault free test.

Table 6. Differences between faulty and normal tests in terms of $T_{A,out,CC}$, T_{RA}, RH_{RA}, T_{SA} and RH_{SA}.

	ID Test	$T_{A,out,CC}$		T_{SA}		RH_{SA}		T_{RA}		RH_{RA}	
		μ (°C)	σ (°C)	μ (°C)	σ (°C)	μ (%)	σ (%)	μ (°C)	σ (°C)	μ (%)	σ (%)
Summer tests	**S1_FF**	15.52	2.57	24.39	3.23	55.17	18.25	26.36	1.03	49.43	3.23
	S2_F1	12.76	0.54	19.61	2.17	55.64	4.70	28.55	0.27	55.39	1.72
	%D	-17.78%	-79.11%	-19.59%	-33.04%	0.85%	-74.25%	8.31%	-73.69%	12.05%	-46.70%
	S1_FF	15.57	2.69	25.08	7.11	53.16	17.57	26.44	1.01	49.19	3.08
	S3_F2	14.82	0.61	18.07	1.48	88.25	12.39	27.42	0.89	49.50	3.55
	%D	-4.81%	-77.18%	-27.94%	-79.17%	66.02%	-29.44%	3.74%	-12.05%	0.63%	15.22%
	S1_FF	15.49	2.63	24.20	7.33	55.98	18.70	26.17	0.80	49.19	3.03
	S4_F3	15.68	2.70	19.21	6.26	67.22	11.87	25.89	0.83	48.07	3.18
	%D	1.22%	2.49%	-20.60%	-14.64%	20.08%	-36.52%	-1.06%	3.51%	-2.29%	5.10%
Winter tests	**W2_FF**	10.77	0.35	17.76	4.92	67.83	17.23	20.20	0.88	50.57	3.35
	W4_F1	17.81	0.97	35.18	0.59	25.27	0.92	19.36	0.38	46.50	1.16
	%D	65.37%	172.97%	98.07%	-87.95%	-62.75%	-94.64%	-4.13%	-56.45%	-8.06%	-65.34%
	W3_FF	9.90	0.60	22.38	5.96	53.16	19.34	20.22	0.78	50.09	3.33
	W5_F2	9.25	0.89	22.98	6.72	53.37	18.78	20.22	0.82	50.04	4.49
	%D	-6.58%	47.29%	2.69%	12.77%	0.39%	-2.93%	0.00%	5.55%	-0.10%	34.58%
	W1_FF	10.86	1.46	20.43	6.18	59.91	17.61	20.20	0.87	50.85	2.75
	W6_F3	10.65	1.57	17.22	5.65	67.35	15.82	20.11	0.91	48.27	1.71
	%D	-1.95%	7.93%	-15.74%	-8.50%	12.42%	-10.18%	-0.41%	3.78%	-5.07%	-37.77%

Table 6 indicates that, with respect to the cases without faults, in the case of the fault 1 (velocity of the supply air fan kept reduced at 20% instead of 50%):

- during summer, the maximum %D in terms of standard deviation is -79.1% for $T_{A,out,CC}$, while the minimum is -33.0% for T_{SA}; the maximum %D in terms of arithmetic mean is -19.6% for T_{SA}, while the minimum is +0.9% for RH_{SA}; during summer, the percentage difference in terms of standard deviation is significant for all the parameters ($T_{A,out,CC}$, T_{RA}, RH_{RA}, T_{SA}, RH_{SA}); the values of %D in terms of arithmetic mean can be assumed as not really relevant for all the parameters ($T_{A,out,CC}$, T_{RA}, RH_{RA}, T_{SA}, RH_{SA});
- during winter, the maximum %D in terms of standard deviation is 173.0% for $T_{A,out,CC}$, while the minimum is -56.5% for T_{RA}; the maximum %D in terms of arithmetic mean is 98.1% for T_{SA}, while the minimum is -4.1% for T_{RA}; during winter, the percentage difference in terms of standard deviation is relevant for all the parameters ($T_{A,out,CC}$, T_{RA}, RH_{RA}, T_{SA}, RH_{SA}); the %D in terms of arithmetic mean is significant only for $T_{A,out,CC}$, T_{SA} and RH_{SA}.

Table 6 also shows that, in comparison to the cases without faults, in the case of the fault 2 (velocity of the return air fan kept reduced at 20% instead of 50%):

- during summer, the maximum %D in terms of standard deviation is -79.2% for T_{SA}, while the minimum is -12.1% for T_{RA}; the maximum %D in terms of arithmetic mean is 66.0% for RH_{SA}, while the minimum is -0.6% for RH_{RA}; during summer, the values of %D in terms of standard deviation are significant for $T_{A,out,CC}$, T_{SA} and RH_{SA} only; the values of %D in terms of arithmetic mean can be assumed relevant only for T_{SA} and RH_{SA};
- during winter, the maximum %D in terms of standard deviation is 47.3% for $T_{A,out,CC}$, while the minimum is -2.9% for RH_{SA}; the maximum %D in terms of arithmetic mean is -6.6% for $T_{A,out,CC}$,

while the minimum is 0.0% for T_{RA}; during winter, the values of %D in terms of standard deviation are significant only for $T_{A,out,CC}$ and RH_{RA}; the values of %D in terms of arithmetic mean can be assumed as negligible for all the parameters ($T_{A,out,CC}$, T_{RA}, RH_{RA}, T_{SA}, RH_{SA}).

Finally, table 6 demonstrates that, with reference to the cases without faults, in the case of fault 3 (the opening percentage of the valve regulating the flow to the humidifier has been kept closed):

- during summer, the maximum %D in terms of standard deviation is -36.5% for RH_{SA}, while the minimum is 2.5% for $T_{A,out,CC}$; the maximum %D in terms of arithmetic mean is -20.6% for T_{SA}, while the minimum is -1.1% for T_{RA}; during summer, the values of %D in terms of standard deviation are significant only for RH_{SA}; the values of %D in terms of arithmetic mean are relevant for T_{SA} and RH_{SA} only;
- during winter, the maximum %D in terms of standard deviation is -37.8% for RH_{RA}, while the minimum is 3.8% for T_{RA}; the maximum %D in terms of arithmetic mean is -15.7% for T_{SA}, while the minimum is -0.4% for T_{RA}; during winter, the value of %D in terms of standard deviation is significant only for RH_{RA}; the values of %D in terms of arithmetic mean can be assumed as not really relevant for all the parameters ($T_{A,out,CC}$, T_{RA}, RH_{RA}, T_{SA}, RH_{SA}).

For each type of fault and parameter, a performance index has been assigned in table 7 with the following sings: "+" indicates that the fault causes substantial positive changes (greater than 20%) of %D; "-" indicates that the fault causes substantial negative changes (greater than -20%) of %D; "0" indicates that the fault causes not substantial changes (between -20% and 20%) of %D.

Table 7. Symptoms' relevance of the faults.

	Fault	**$T_{A,out,CC}$**		**T_{SA}**		**RH_{SA}**		**T_{RA}**		**RH_{RA}**	
	name	**μ**	**σ**	**μ**	**σ**	**μ**	**σ**	**μ**	**σ**	**μ**	**σ**
Summer tests	**F1**	0	-	0	-	0	-	0	-	0	-
	F2	0	-	-	-	+	-	0	0	0	0
	F3	0	0	-	0	+	-	0	0	0	0
Winter tests	**F1**	+	+	+	-	-	-	0	-	0	-
	F2	0	+	0	0	0	0	0	0	0	+
	F3	0	0	0	0	0	0	0	0	0	-

6. Conclusions

The symptoms of 3 typical faults related to the supply/return air fans and the humidifier valve of a typical HVAC system have been preliminarily assessed based on measured data. The preliminary analysis highlighted that: a velocity of the supply air fan reduced at 20% (instead of 50%) mainly affects the values of $T_{A,out,CC}$, T_{SA} and RH_{SA} during winter; a velocity of the return air fan reduced at 20% (instead of 50%) significantly influences the values of T_{SA} and RH_{SA} during summer; the impact is also relevant with reference to the values of RH_{SA} during summer in the case of the humidifier valve is kept fully closed. In the future the authors would like to perform additional fault free and faulty tests with the aims of (i) extending the analysis of the faults investigated in this work under different operating scenarios, as well as (ii) assessing the impact of new faults regarding sensors, controlled devices, equipment and controllers. In addition, it would be desirable to develop and experimentally validate a simulation tool able to predict the behaviour of the HVAC system in order to assist future researches on AFDD methods.

7. References

[1] Li B, Rowe A, Wild P 2021 Energy code effectiveness on GHG emission mitigation for single-family houses in Canada *J. Clean. Prod.* **299**
[2] Cao X, Dai X, Liu J 2016 Building energy-consumption status worldwide and the state-of-the-art technologies for zero-energy buildings during the past decade *Energy Build.* **128**
[3] Roselli C, Sasso M, Tariello F 2019 Assessment of a solar PV-driven desiccant-based air handling unit with different tracking systems *Sustain. Energy Technol. Assess.* **34**
[4] Yan K, Zhong C, Ji Z, Huang J 2018 Semi-supervised learning for early detection and diagnosis of air handling unit faults *Energy Build.* **181**
[5] Lin G, Kramer H, Granderson J 2020 Building fault detection and diagnostics: Achieved savings, and methods to evaluate algorithm performance *Build. Environ.* **168**
[6] Rosato A, Guarino F, Filomena V, Sibilio S, Maffei L 2020 Experimental calibration and validation of

a simulation model for fault detection of HVAC systems and application to a case study *Energies* **13**

[7] Piscitelli M S, Mazzarelli D M, Capozzoli A 2020 Enhancing operational performance of AHUs through an advanced fault detection and diagnosis process based on temporal association and decision rules *Energy Build.* **226**

[8] Guarino F, Filomena V, Maffei L, Sibilio S, Rosato A 2019 A Review of Fault Detection and Methodologies for Air-Handling Units *Glob. J. Energ. Technol.* **6**

[9] Wen J, Li S 2012 ASHRAE 1312-RP - Tools for evaluating fault detection and diagnostic methods for Air-Handling Units, American Society of Heating, Refrigeration and Air-Conditioning Engineers: Atlanta, GA, USA.

Acknowledgments

This work was undertaken as part of the program “PON FSE-FESR Ricerca e Innovazione 2014–2020” of the Italian Ministry of Education, University and Research, Action I.1 “Dottorati Innovativi con caratterizzazione industriale”.